Chemical Engineering Journal 423 (2021) 130149

Contents lists available at ScienceDirect

Chemical Engineering Journal

journal homepage: www.elsevier.com/locate/cej

Vitamin B12 (Co^{II}) initiates the reductive defluorination of branched perfluorooctane sulfonate (br-PFOS) in the presence of sulfide

Zhuyu Sun [a,b], Dan Geng [a], Chaojie Zhang [b,c,*], Jiabin Chen [b,c], Xuefei Zhou [b,c], Yalei Zhang [b,c], Qi Zhou [c], Michael R. Hoffmann [d]

[a] College of Environmental Science and Engineering, Donghua University, Shanghai, 201620, China
[b] Shanghai Institute of Pollution Control and Ecological Security, Shanghai 200092, China
[c] State Key Laboratory of Pollution Control and Resources Reuse, College of Environmental Science and Engineering, Tongji University, Shanghai 200092, China
[d] Linde-Robinson Laboratories, California Institute of Technology, Pasadena, CA 91125, United States

ARTICLE INFO

Keywords:
Perfluorooctane sulfonate (PFOS)
Reductive defluorination
Vitamin B12 (VB12)
Co^{II} oxidation state
Degradation pathway

ABSTRACT

Due to the extremely high stability of perfluorooctane sulfonate (PFOS), effective defluorination is difficult. Previous studies indicated that PFOS can be decomposed under the catalysis of vitamin B12 (VB12) with strong artificial reductants such as Ti(III)-citrate and nZn^0. In this study, we explored if naturally occurring reductant like sulfide (S^{2-}) could initiate the reaction. In S^{2-}/VB12 system, branched PFOS (br-PFOS) can undergo effective decomposition and defluorination at the temperature of 70 °C and pH greater than 12. The degradation of br-PFOS fits pseudo-first-order kinetic with a rate constant of 0.0984 ± 0.0034 d^{-1} in the presence of 30 mM Na_2S and 300 μM VB12, while linear PFOS (L-PFOS) remained stable during 30 d reaction process. UV–Vis spectral characterization indicates that S^{2-} reduces VB12(Co^{III}) to Co^{II}, which is able to initiate the reductive defluorination. Based on the product analysis, HF/2F elimination followed by C–C scission is the dominant degradation pathway of br-PFOS instead of stepwise H/F exchange. The primary products include F^- and polyfluorinated sulfonates and carboxylates. The degradation of br-PFOS is strongly dependent on temperature due to a relatively high apparent activation energy of 62.86 kJ/mol. Strong alkaline condition can greatly enhance the decomposition efficiency since S^{2-} is the primary reactive form. This study provides new insights into the VB12-catalyzed defluorination of PFOS and a feasible approach for future natural or engineered remediations of br-PFOS.

1. Introduction

Perfluorooctane sulfonate (PFOS, $C_8F_{17}SO_3^-$) is a useful anthropogenic chemical that has unique physico-chemical properties such as superior surface-tension-lowering properties, water and oil repellency and chemical and thermal stability [1,2]. Since the late 1940 s, perfluoroalkyl substances (PFASs) including perfluorooctanoic acid (PFOA) and PFOS have been extensively manufactured and widely used in various industrial and commercial applications, such as metal plating and cleaning, coating formulations, fire-fighting foams, varnishes, vinyl polymerization, oil and lubricants, water repellents for leather, paper and insecticide [3,4]. The Swedish Chemicals Agency (2015) estimated that more than 4000 PFASs have been synthesized so far, with more than 2000 on the global market [5]. Those PFASs have high persistence, bioaccumulation and toxicity, and has been ubiquitously detected in the global environmental and biological matrices [2,6], thus posing great risks to environment, biota and human health [7,8]. However, due to the extremely high stability of C–F bond (~116 kcal/mol, almost the strongest in nature [2]), defluorination of PFASs is not an easy task [9–11]. Current advanced treatments include sonochemical destruction [12], electrochemical oxidation [13], radiochemical irradiation [14], microwave-hydrothermally induced persulfate oxidation [15], hydrated electron based photoreduction [16], elimination by zerovalent iron in subcritical water [17] and plasma chemical degradation [18]. However, most of these technologies are cost-intensive, and require specific equipment or harsh reaction conditions, which may limit their large-scale implementation. Furthermore, although great efforts have been made to explore the potential natural/microbial degradation of those perfluorinated substances, PFASs are extremely microbiologically inert and persistent under most aerobic and anaerobic cases. Therefore,

* Corresponding author.
E-mail address: myrazh@tongji.edu.cn (C. Zhang).

https://doi.org/10.1016/j.cej.2021.130149
Received 21 January 2021; Received in revised form 24 April 2021; Accepted 27 April 2021
Available online 4 May 2021

developing a feasible PFOS decomposition technology is still urgent and desirable.

Vitamin B12 (VB12) is a complex organometallic cofactor which plays crucial roles in several biological processes. VB12 also shows high catalytic reactivities towards various halogenated compounds such as carbon tetrachloride [19], tetrachloroethylene [20], hexachlorobenzene [20], 2,3,4,5,6-pentachlorobiphenyl [21], 2,6-dichlorophenol [22], 2,2′,4,4′-tetrabromodiphenyl ether [23], etc. Anaerobic microbes containing B12-dependent reductive dehalogenases play important roles in the detoxification of aromatic and aliphatic chlorinated organics, such as chlorinated phenols, chlorinated ethenes, and PCBs [24,25]. In 2008, **Ochoa-Herrera et al.** reported for the first time that vitamin B12 can catalyze the reductive defluorination of PFOS with Ti(III)-citrate as the bulk reductant [26]. In the Ti(III)-citrate/VB12 system, branched PFOS (br-PFOS) can be effectively decomposed with a pseudo-first-order kinetic rate constant of 0.0204 h^{-1} (36 mM Ti(III)-citrate; 260 μM VB12; 70 °C; pH 9.0) [26]. Subsequently **Park et al. (2017)** demonstrated that br-PFOS can be effectively transformed under VB12-nZn^0 and VB12-nFe^0 systems as well, with the generation of F^- and polyfluoroalkyl products [27]. Then **Liu et al. (2018)** investigated the structure–reactivity relationships within branched per- and polyfluoroalkyl substances (PFASs) under VB12/Ti(III)-citrate system [28]. In those previous studies the electron donors used were all artificially prepared strong reductants such as Ti(III)-citrate or nanoscale zero-valent metals, which are expensive for future engineering applications. Therefore, we wondered if VB12 catalytic system can work with more naturally occurring or accessible reductants for efficient degradation and defluorination of PFOS. Furthermore, the catalytic mechanism of VB12 needs further investigation as well, such as the oxidation state of Co (Co^{III}, Co^{II}, Co^{I}), which determines the nucleophilicity and reactivity of VB12, and affects the transformation products of the contaminants [29].

Sulfide (S^{2-}) is a naturally occurring reductant that is commonly found in hypoxic environments such as landfill leachate, thermal springs, hazardous subsurface waste plumes, anoxic estuarine porewaters, salt marshes, etc., at the concentration levels ranging from 0.2 μM to 12 mM [30–33]. Sewage and industrial wastewaters from e.g. petrochemical, tanneries and textile also contain large amounts of S^{2-} [34–36]. Reductive sulfide species such as H_2S, HS^-, S_n^{2-}, S^{2-} play important roles in the abiotic transformation of halogenated organics serving either as nucleophile [33,37] or as bulk electron donors [38–40]. For instance, the natural transformation of pentachloroethane and hexachloroethane in anoxic hypolimnion was predominately resulted from abiotic dehalogenation [41]. Therefore, considering S^{2-} is a common natural reductant in anoxic environment, its role in PFASs degradation needs evaluating, either as a direct nucleophile, or as a bulk reductant for some electron-transfer mediators such as VB12.

Therefore in the present study we investigated the degradation and defluorination of PFOS with VB12 as the catalyst and S^{2-} as the bulk reductant. S^{2-} has a comparable redox potential with Ti(III)-citrate and Fe^0 (E° (S^{2-}/S) = − 0.476 V; E° (Ti(III)-citrate/Ti(IV)-citrate) = − 0.48 V; E° (Fe^0/ Fe^{2+}) = − 0.447 V). The electron transfer mechanism was elucidated by characterizing the oxidation state of Co in VB12 molecule with ultraviolet–visible (UV–Vis) spectra. Furthermore, the possible degradation pathways of PFOS were proposed based on the identification and quantification of aqueous intermediate products. The effects of environmental parameters including temperature, pH and the concentrations of S^{2-} and VB12 were also evaluated.

2. Materials and methods

2.1. Chemicals

Perfluorooctanesulfonic acid (PFOS, ~40% in water), vitamin B12 (≥98.0%), sodium sulfide nonahydrate ($Na_2S{\cdot}9H_2O$, ≥98.0%) and HPLC grade methanol (≥99.9%), were purchased from Sigma-Aldrich Chemical Co. (St. Louis, Mo, USA). Titanium(III) chloride ($Ti(III)Cl_3$, 20% in 3% HCl) was acquired from *J&K* scientific Co. (Beijing, China). Dithiothreitol (DTT, 99%) and L-cysteine (98%) were purchased from Aladdin Bio-Chem Technology Co. (Shanghai, China). Hydrochloric acid (HCl, 36%-38%), triammonium citrate (≥99.0%) and sodium fluoride (NaF, ≥99.0%) were obtained from Sinopharm Chemical Reagent Co. (Shanghai, China). HPLC grade ammonium acetate (97.0%) was purchased from TEDIA (Fairfield, OH, USA). Sodium perfluoro-1-[1,2,3,4-$^{13}C_4$]octanesulfonate (MPFOS, ≥99%, $^{13}C_4$) acquired from Wellington Laboratories Inc. (Guelph, ON, Canada) was used as the internal standard for the quantification of PFOS. Milli-Q water and deionized water were used throughout the whole experiment.

2.2. Reductive defluorination

Reductive defluorination of technical PFOS by VB12 and S^{2-} was conducted in batch assays under anoxic condition. All experiments were set up in triplicate in an anaerobic glove box. 100 mL serum bottle sealed with butyl rubber stoppers and aluminum crimp caps were used as the reaction container and all serum bottles were wrapped with aluminum foil to prevent VB12 decomposition by light. Deionized water was prebubbled with N_2 gas (99.99%) for 30 mins before being added to the vials. The initial solution pH was adjusted with 0.5 M HCl or NaOH without buffer addition. The serum bottles were placed in a shaking bath with an oscillation frequency of 120 rpm. After various time intervals, samples of the liquid were taken for analysis after dilution and filtration through 0.22 μm nylon filter (ANPEL Laboratory Technologies, Shanghai, China). All sample preparation and treatment were conducted in the anaerobic chamber.

2.3. Analytical methods

The concentration of PFOS was determined by high-performance liquid chromatography/tandem mass spectrometry (HPLC − MS/MS, TSQ^{TM} Quantum Access^{TM}, Thermo Finnigan, San Jose, CA, USA). Fluoride was quantified by ion Chromatography (Dionex, ICS-3000, Thermo Fisher Scientific, USA) equipped with a conductivity detector. The aqueous-phase intermediates/products were detected by an Agilent (1290) ultra HPLC (UPLC) with an Agilent Quadrupole Time of Flight (QTOF) 6550 mass spectrometer. More detailed information is available in the **SI**.

2.4. Spectroscopic measurements

Spectroscopic measurements were conducted to characterize the oxidation state of the cobalt-center in VB12 during the reaction process. After various time intervals, samples were added to a 1 cm quartz cuvette with a gas-tight syringe after dilution and filtration. The cuvette was sealed with a butyl rubber stopper and sealing film. After all sample preparation and treatment done in anaerobic chamber, spectra were immediately recorded at room temperature with a UNICO spectrophotometer (UV-2800, UNICO, USA).

2.5. Calculations

The PFOS decomposition degree is reflected by the degradation ratio and defluorination ratio, which are defined as follows:

$$\text{Degradation ratio} = \frac{[\text{PFOS}]_0 - [\text{PFOS}]_t}{[\text{PFOS}]_0} \times 100\%$$

$$\text{Defluorination ratio} = \frac{[F^-]_t}{[\text{PFOS}]_0 \times 17} \times 100\%$$

Where $[PFOS]_0$ and $[PFOS]_t$ are the PFOS concentrations at the start of the reaction and at the reaction time t, respectively. $[F^-]_t$ refers to the concentration of fluoride ions at time t.

3. Results and discussion

3.1. Reductive degradation and defluorination of PFOS by S^{2-}/VB12 system

The catalytic reductive degradation and defluorination of 300 μM technical PFOS was conducted in the presence of 30 mM Na_2S and 300 μM VB12 at the temperature of 70 °C under anoxic condition. The initial solution pH was 12.3 (unadjusted) due to the hydrolysis of S^{2-}. In order to investigate the effects of S^{2-} and VB12, two control experiments were carried out. The degradation and defluorinaiton of technical PFOS under different conditions are shown in Fig. 1 **(a, b)**. For the treatment experiment, 31.5% of the initial technical PFOS was decomposed in 30 d in the presence of both S^{2-} and VB12, with a 30-d defluorination ratio of 18.9%. While for the two control experiments, the 30-d degradation and defluorination ratios of technical PFOS were all negligible (3.76% and 2.82% for Na_2S + PFOS, and 0.86% and 0.35% for VB12 + PFOS). This is because in the absence of electron donors, i.e. S^{2-}, VB12 is in the highest oxidation state of Co^{III}, which has no nucleophilicity toward PFOS. Only when Co^{III} is reduced to Co^{II} or Co^{I} can VB12 initiate the reductive dehalogenation. While in the absence of VB12, the reducing strength of S^{2-} under the experimental condition is insufficient for effective degradation and defluorination of PFOS. Therefore, different from those chlorinated or brominated compounds such as carbon tetrachloride [42] and hexachloroethane [41], S^{2-} alone cannot decompose PFOS effectively, which is mainly due to the high energy of C − F bond (~110 kcal/mol), the strong electronegativity of F (4.0) and the extreme chemical stability of the perfluoroalkyl chain. Therefore, S^{2-} and VB12 are both essential for effective PFOS decomposition.

Moreover, many PFASs exist as families of isomers due to branching of the main C backbone [43]. For instance, the electrochemical fluorination process produces a mixture of branched and linear isomers, with a rough proportion of 70% to 80% linear and 20% to 30% branched in the case of PFOS and PFOA [44,45]. The linear and branched isomers behave differently in the environment matrices [46,47] and have different toxicity effects to the biota [48–50]. In our study, the linear and branched PFOS isomers also showed different degradation efficiencies and kinetics (Fig. 1**c, d**). According to the peak areas of HPLC-MS/MS spectra, the technical PFOS used in our study consists of 36.1 ± 2.3% br-PFOS and 63.9 ± 2.0% linear PFOS (L-PFOS) (**Fig. S1, SI**). In the S^{2-}/VB12 system, only br-PFOS isomers could be degraded, with the 30-d degradation and defluorination ratios of 86.2% and 52.2%, respectively. The degradation of br-PFOS fits pseudo-first-order kinetics, with an apparent rate constant (k) of 0.0984 ± 0.0034 d^{-1}. No significant removal of L-PFOS was observed during the 30-d reaction process. This result is consistent with those obtained in Ti(III)-citrate/VB12 system [26] and nZn^0/VB12 system [27], while the reasons are still under debate. **Park et al.** think that the absence of L-PFOS transformation by

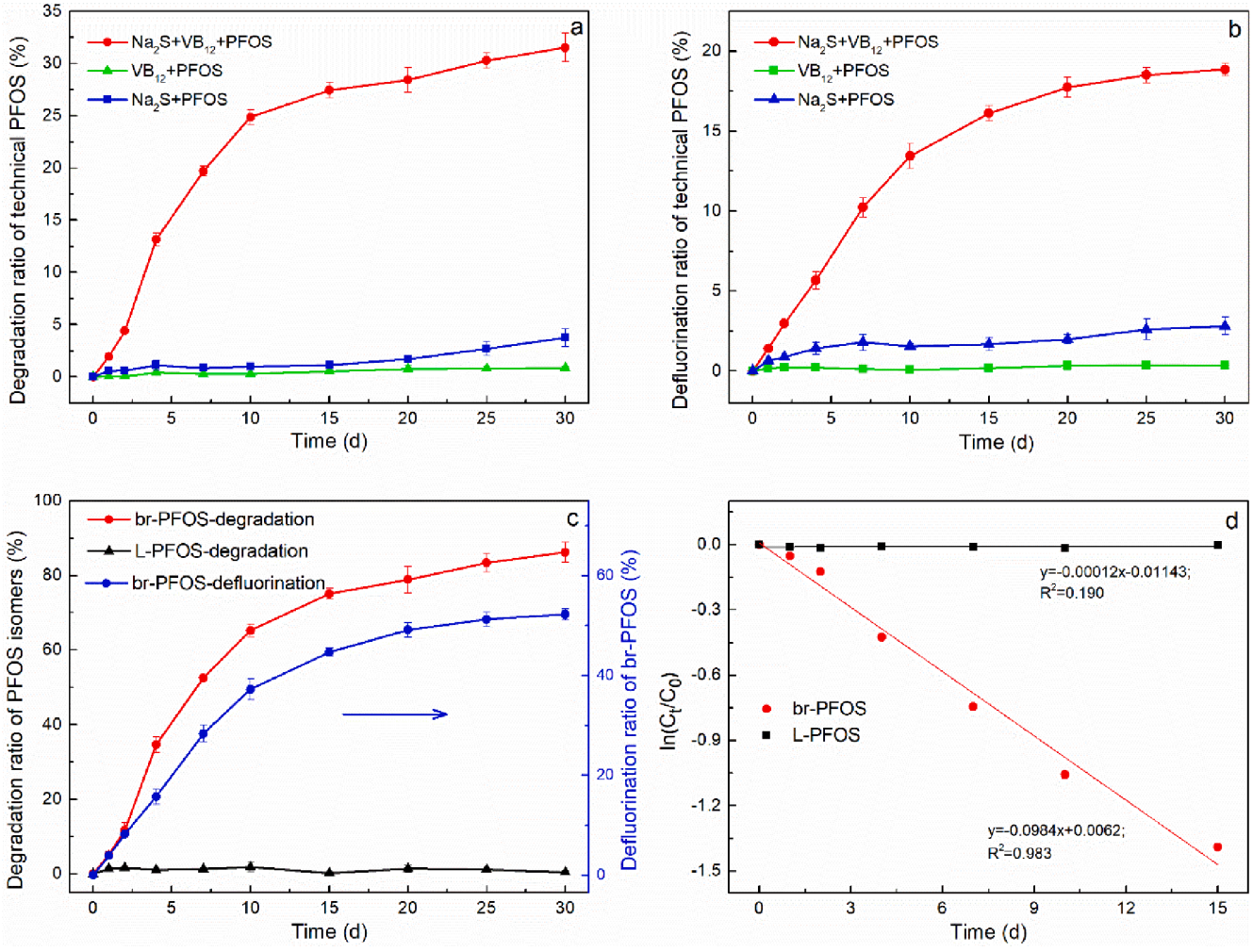

Fig. 1. The time profiles of technical PFOS degradation (**a**) and defluorination (**b**) under different conditions, and the degradation ratios (**c**) and kinetics (**d**) of PFOS isomers. The treatment experiment condition: PFOS (300 μM), Na_2S (30 mM), VB12 (300 μM), 70 °C, pH = 12.3 (unadjusted), anoxic; the 1st control experiment (without VB12): PFOS (300 μM), Na_2S (30 mM), 70 °C, pH = 12.3 (unadjusted), anoxic; the 2nd control experiment (without Na_2S): PFOS (300 μM), VB12 (300 μM), 70 °C, pH = 12.3, anoxic. Error bars represent standard deviations of triplicate assays.

VB12 is possibly due to the inability of L-PFOS to complex with VB12 rather than an activation energy issue [27]. However, **Liu et al.** believe that the extent of PFAS defluorination is determined by the C − F bonding environment and the bond dissociation energies (BDEs) [28]. Therefore, further studies are needed to reveal the underlying isomer-specific catalytic mechanisms in VB12 system. Besides VB12, defluorination of PFSAs with hydrated electrons also shows great structural dependence [51]. For instance, br-PFOS decomposed with a first-order reaction rate constant of 0.0806 min^{-1}, while that of L-PFOS was only 0.0175 h^{-1} [52]. Furthermore, the rate constant of br-PFOS degradation obtained in the S^{2-}/VB12 system of the present study (0.0984 ± 0.0034 d^{-1}, under the conditions of 30 mM Na_2S, 300 μM VB12, 70 °C and unadjusted pH of 12.3) is much lower than the values obtained in the Ti (III)-citrate/VB12 system (0.49 d^{-1}, under the conditions of 36 mM Ti (III)-citrate, 260 μM VB12, 70 °C and pH 9.0) [26] and in the nZn^0/VB12 system (3.35 d^{-1}, 1.39 d^{-1} and 0.37 d^{-1} for 6-PFOS, 5-PFOS, 3&4-PFOS, respectively, under the conditions of 20 g/L nZn^0, 400 μM VB12; 90 °C and pH 10.4) [27]. This may be attributed to the VB12 form changes in the presence of different reductants, which is discussed in **section 3.2**.

3.2. The oxidation state changes of VB12(Co) and the electron transfer mechanism in S^{2-}/VB12 system

The oxidation state changes of Co in VB12 molecule were characterized by a UV–Vis spectrometer. The spectra under different experimental conditions after 1-d reaction are shown in Fig. 2**a**. In the absence of S^{2-} (VB12 + PFOS), VB12 was in the oxidation state of Co^{III}, with characteristic peaks appearing at 278, 361 and 550 nm [53]. By adding 30 mM Na_2S, the characteristic peaks for Co^{III} disappeared along with the concomitant appearance of Co^{II} peaks at 310 and 470 nm [53], indicating that cyanocobalamin(III) was reduced to cobalamin(II) via an one-electron transfer from S^{2-}. The characteristic peak for Co^{I} at 390 nm [53] didn't appear during the whole reaction process, indicating that S^{2-} is just capable of reducing VB12 to the Co^{II} state, whereas further reduction to Co^{I} cannot be realized. Previous studies indicated that br-PFOS could be effectively decomposed by the supernucleophile VB12 (Co^{I}) in the presence of Ti(III)-citrate [26] or nanoscale zero-valent metals like nZn^0 and nFe^0 [27]. The results in our study demonstrate that br-PFOS can be effectively decomposed by VB12(Co^{II}), a much weaker nucleophile compared to VB12(Co^{I}). This implies that br-PFOS may undergo efficient degradation in a relatively high redox potential condition with VB12(Co^{II}) as the reactive catalyst, which makes the degradation of br-PFOS more easily achieved in some physiological or natural environments. However, it's also noteworthy that either in the presence of Co^{I} or Co^{II}, efficient defluorination of br-PFOS requires a high temperature, indicating a high activation energy requirement for the cleavage of C − F bond even though in the presence of a catalyst. Some studies indicated that the VB12 dependent enzymes can accelerate the electron transfer and reduction of Co, transform VB12 to active coenzyme forms, stabilize Co^{II} and Co^{I} states and facilitate the carbon − halogen bond cleavage [54–56]. Other studies reported that some zerovalent metals or carbon materials can activate the C − F bond of PFASs. Therefore, exploring approaches that can further lower the dissociation energy of C − F bond is of great significance for VB12 system.

The UV–Vis spectral changes of the S^{2-}/VB12 system recorded as the reaction proceeded are shown in Fig. 2**b**. Initially, VB12 was in the oxidation state of Co^{III} with its characteristic peaks at 278, 361 and 550 nm, indicating that the electron transfer from S^{2-} to VB12 under ambient temperature condition is not instantaneous, which is different from the Ti(III)-citrate/VB12 system (**Fig. S2, SI**). After mixing for 4 h under a stationary state at ambient temperature, VB12 (Co^{III}) was gradually reduced to Co^{II}. When reacting at 70 °C for 1 day, almost all Co^{III} was reduced to Co^{II}. During the reaction period from 1 d to 30 d, no significant spectral changes were observed (**Fig. S3, SI**), indicating that the electron donor (S^{2-}) was in excess. The consumption of S^{2-} during

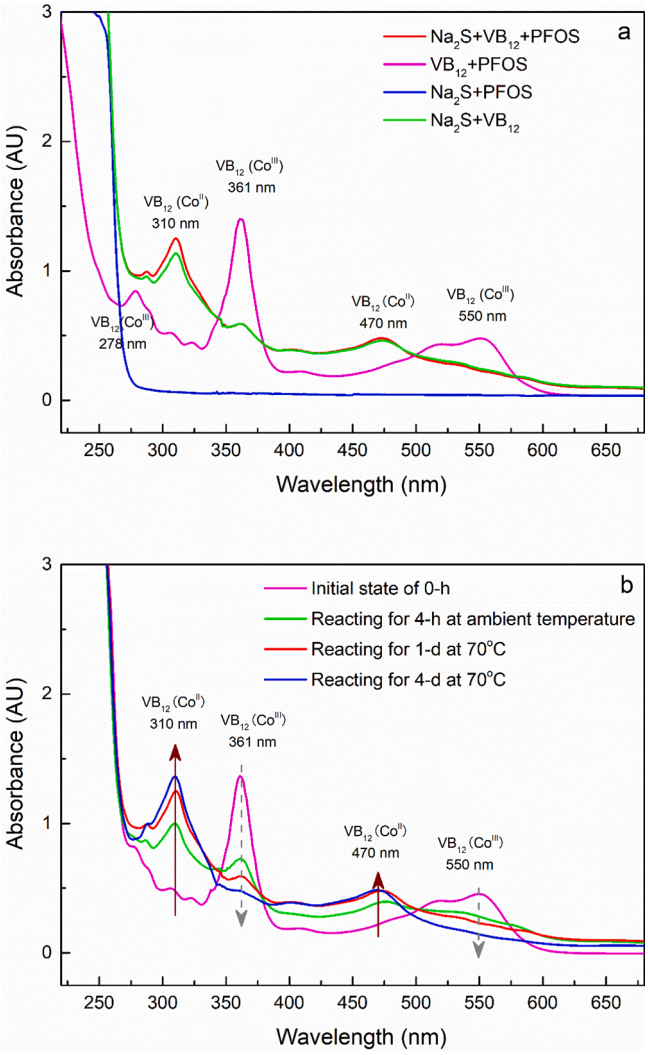

Fig. 2. UV–Vis absorption spectra of solutions under different conditions after 1-d reaction (**a**). The conditions were the same as Fig. 1. The UV–Vis absorption spectral changes of the treatment experiment during the reaction process (**b**).

the reaction process is shown in **Fig. S4** (**SI**). Based on the spectral results and above discussion, a schematic diagram showing the electron transfer mechanism in S^{2-}/VB12 system is illustrated in Fig. 3. The reduction of VB12 by S^{2-} is speculated to occur via the following three

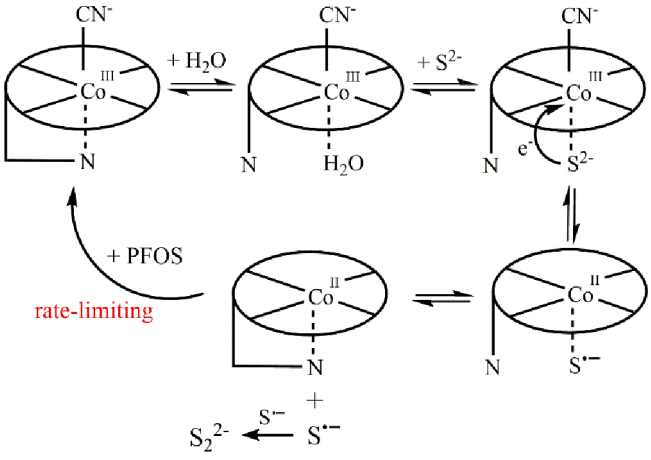

Fig. 3. The proposed catalytic mechanism of VB12.

steps. i) Firstly, the 5,6-dimethylbenzimidazole (DMBI) at the bottom α axial position at the fifth coordination site of Co is replaced by a water molecule to generate the base-off form of cobalamin (i.e. the dissociation of DMBI) [57]. ii) Then the high mobility of water ligand facilitates its rapid substitution by S^{2-} and upon the rapid complexation with S^{2-}, electron transfer occurs to reduce Co^{III} to Co^{II}. The resulting sulfide radical remains within the inner coordination sphere of the resulting Co^{II}. Since Co^{II} tends to be pentacoordinated, cyanide binds weakly to the Co^{II} corrins and therefore leaves the complex. iii) Subsequently, the sulfide radical may react with a second molecule of $S^{\bullet-}$, which leads to a shift in the equilibrium toward pentacoordinated base-on Cbl^{II} form. Based on the above discussion, S^{2-} reduces VB12 from Co^{III} to Co^{II} via an inner single electron transfer mechanism, whereas Ti(III)-citrate can reduce VB12 from Co^{III} to Co^{I}, probably via a faster outer electron transfer process. This explains the slower reduction rate of VB12(Co^{III}) and the lower degradation rate of PFOS by S^{2-}/VB12 system than by Ti (III)-citrate/VB12 system, in the presence of comparable concentration levels of the reductants and VB12 and at the same reaction temperature of 70 °C.

In conclusion, VB12 (Co^{III}) can be effectively reduced by S^{2-} at ambient temperatures and VB12 (Co^{II}) can initiate the degradation and defluorination of br-PFOS, with the latter one as the rate-limiting step. A plausible explanation for the rate limitation is that the high C − F bond dissociation energy of br-PFOS makes the nucleophilic substitution reaction by VB12 proceed slowly. Moreover, in order to validate the effect of VB12 (Co^{II}), we utilized other two common reagents (dithiothreitol and L-cysteine) that can also effectively reduce VB12 (Co^{III}) to VB12 (Co^{II}) under alkaline conditions. According to the results shown in **Fig. S5** (**SI**), dithiothreitol and L-cysteine have comparable efficiencies with S^{2-}. Base on the spectral and color changes (**Fig. S6**, **SI**), VB12 was reduced to Co^{II} state in the presence of these reductants. Therefore, with proper reductant, VB12 in the Co^{II} state can successfully initiate the degradation and defluorination of br-PFOS.

3.3. Reductive degradation products of PFOS by S^{2-}/VB12 system.

The aqueous organic intermediates/products generated from the degradation of PFOS in S^{2-}/VB12 system were detected by UPLC/QTOF-MS and possible products are summarized in **Table S1** in the **SI**, along with their MS/MS fragments. Based on the peak area and the abundance in MS, most intermediates with high intensities were polyfluorinated sulfonates with a MS/MS fragment of around 79.958 Da. Initial PFOS degradation intermediates identified included $C_8F_{15}SO_3^-$ (mass of 461), which was presumably generated via the H/F exchange of br-PFOS (498) followed by HF elimination, or via a direct 2F β elimination. The intermediate with *m/z* 477 was assigned to $C_8F_{15}OSO_3^-$, which was possibly formed via the nucleophilic substitution of F by OH^- (to generate the alcohol intermediate of $C_8F_{16}OHSO_3^-$) and subsequent HF elimination. These intermediates indicate that H/F exchange, 2F β elimination, and nucleophilic substitution of F by OH^- are all possible initial defluorination steps that may occur in S^{2-}/VB12 system. The high abundance of $C_8F_{15}SO_3^-$ (461) instead of $C_8HF_{16}SO_3^-$ (481) implies the dominance of 2F β elimination over H/F exchange, which may be resulted from the strong alkaline condition. At high pH values, there will be an increased concentration of OH^-, a lower redox potential of VB12 and stronger nucleophilicity of VB12 and OH^-. This is also consistent with the results in e_{aq}^- system that high pH condition favors deep defluorination of PFAAs by cleaving multiple strong C − F bonds [58]. After the first defluorination step, several short chain polyfluorinated sulfonates were detected, implying that the initial intermediates, such as $C_8F_{15}SO_3^-$ (461) underwent further C − C scission. These short chain polyfluorinated sulfonates mainly include C4- (281), C3– (231), C2– (181) based 1H- polyfluorinated sulfonates. In addition, multitudinous intermediates/products were detected in the mass range of 179–289. Most of them were identified as short chain polyfluorinated carboxylates because of loss of $–COO^-$ (44) in the MS/MS fragments compared with the parent ions. These short chain polyfluorinated carboxylates were possibly derived from C − C scission or C − S fission. Except trifluoroacetic acid (TFA), no short chain perfluoroalkyl carboxylates were detected including PFOA, indicating that defluorination occurred before C − C scission and C − S fission. To be noted, similar with **Bentel et al.**, a small portion of shorter chain PFSAs including PFHpS, PFHxS, and PFBS was found as impurities in the commercial PFOS in our study [51]. However, the short chain polyfluorinated sulfonates were still considered as the intermediates derived from PFOS defluorination because most of them have much higher abundances than the PFSAs impurities.

Based on the product analysis, in addition to the PFOS degradation and F^- formation, possible degradation pathways of br-PFOS are shown in Fig. 4. Herein, 6-PFOS was used as an example, while other branched isomers may undergo similar degradation pathways since peaks of product isomers were detected in the chromatogram. Basically, defluorination of br-PFOS occurs via H/F exchange, 2F β elimination, HF elimination and nucleophilic substitution by OH^-. The initial defluorination site may be located in the tertiary C − F bond adjacent to two trifluoromethyl groups ($-CF_3$) because tertiary C − F bond has a relatively low bond dissociation energy (BDE) [28]. The occurrence of α-H or alkene C = C double bond as a result of the H/F exchange or 2F/HF elimination can further decrease the BDEs of adjacent C-F bond, thus rendering br-PFOS able to undergo a stepwise defluorination. However, after the initial defluorination, the C − C bond scission were believed to be the dominant pathway due to the remarkably high abundance of 1H-polyfluorinated sulfonates (**Fig. S7&S8, SI**). Moreover, based on the formation of shorter chain carboxylates, C-S bond were also possibly cleaved, which may lead to the formation of polyfluorinated alcohols ($C_xH_yF_zOH$) first, and then $C_xH_yF_zCOF$ via HF elimination or $C_xH_yF_zCHO$ via 2F elimination. $C_xH_yF_zCOF$ then underwent hydrolysis to form $C_xH_yF_zCOO^-$ and F^- (the *DHEH* pathway [51,59]). However, due to the complexity and diversity of these polyfluorinated intermediates, their MS and MS/MS fragments are difficult to be assigned to. The MS/MS spectra of some primary polyfluorinated sulfonate products and polyfluorinated carboxylate products are shown in **Fig. S9** and **Fig. S10**, respectively. The C − C and C − S bond scission may be derived from the single electron transfer from VB12 (Co^{II}). **Gu et al.** indicated that after the electron was transferred to PFOS, it would localize in the C − C antibonding orbitals of PFOS ($C8F17SO3\bullet^{2-}$) [60]. They also suggested a lower bond energy and dissociation energy of C − S bond [60]. Therefore, the electron transfer from VB12 (Co^{II}) and its consequent delocalization could result in the C − C and C − S bond scission of PFOS. Overall, the product distribution in this study revealed that the degradation pathways of br-PFOS in the S^{2-}/VB12 system were different from those in the VB12-nZn^0 system [27]. In VB12-nZn^0 system, br-PFOS undergoes a series of F replacement by H with $C_8H_8F_5SO_3^-$ as the terminal product [27]. No shorter chain intermediates (except $C_7HF_{16}SO_3^-$) were identified [27]. While in our study, a series of short chain polyfluorinated sulfonates and carboxylates were detected. The difference in the degradation pathway can be ascribed into two aspects: (1) the different oxidation states of Co and different reducing environment. The S^{2-} reduces VB12 to Co^{II}, while nZn^0 can reduce VB12 to Co^{I}. **Lewis et al.** reported that the dehalogenation products of carbon tetrachloride catalyzed by VB12 were dependent on the Co form of VB12 and/or the impact of the reductant on reactive intermediates [29]. (2) The different pH conditions. **Bentel et al.** indicated that in the e_{aq}^- system, high pH condition favors deep defluorination and increases the probability of taking *DHEH* pathway [58]. Therefore, compared with the pH 9.0 condition of VB12-nZn^0 system, the strong alkaline condition of S^{2-}/VB12 system (pH greater than 12.0) may enhance the *DHEH* pathway, thus facilitates the conversion of br-PFOS into shorter chain polyfluorinated intermediates/products. Due to the diversity of br-PFOS and polyfluorinated intermediates, further systematic products study are needed to reveal the underlying defluorination pathways and mechanisms.

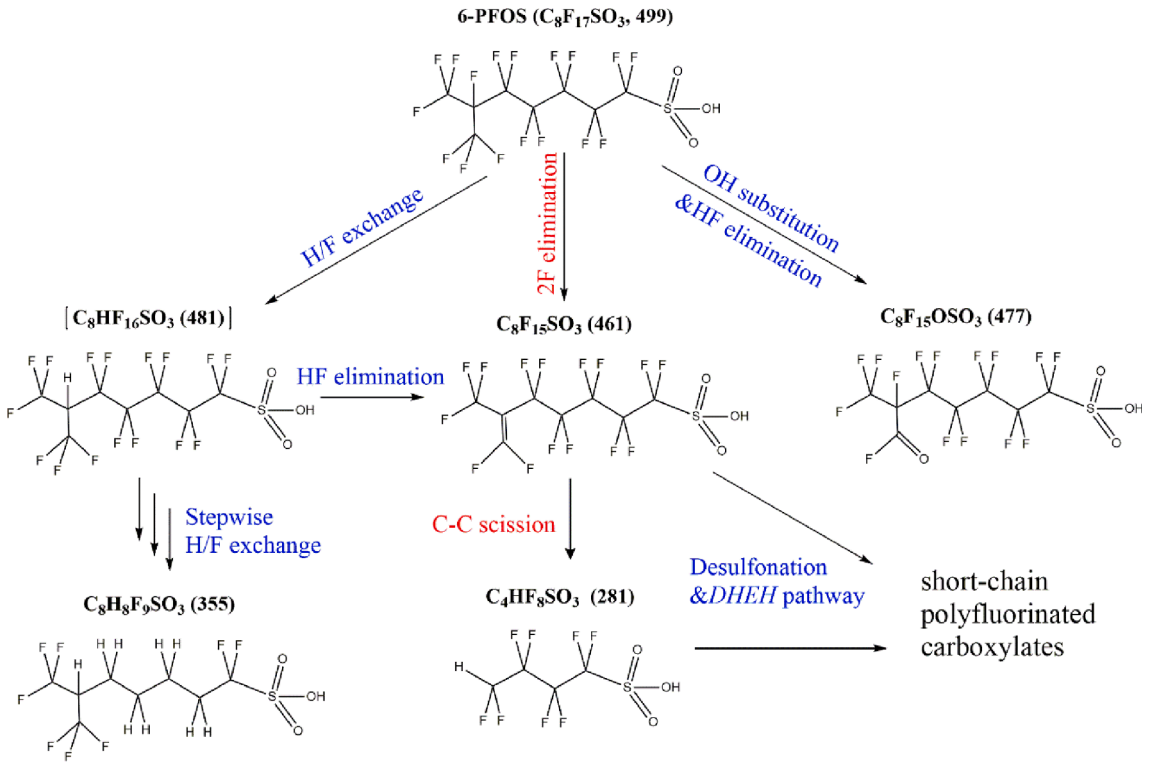

Fig. 4. A proposed br-PFOS degradation pathway based on observed mass, MS/MS fragmentation and peak areas of defluorination intermediates/products. 6-PFOS was used as an example. Structures of the intermediates/products can vary with different isomers. The product in brackets is a speculative intermediate. The process in red is considered as the dominant pathway. (For interpretation of the references to color in this figure legend, the reader is referred to the web version of this article.)

3.4. Effects of environmental parameters

3.4.1. Effect of temperature

The effect of temperature in the range 30–90 °C on the degradation and defluorination of br-PFOS is shown in Fig. 5 **(a, b)**. Obviously the catalytic reductive reaction was very sensitive to the temperature. The 20-d degradation ratio of br-PFOS increased remarkably from 5.8% at the temperature of 30 °C to 93.5% at the temperature of 90 °C. The 20-d defluorination ratio of br-PFOS also increased from 3.4% (30 °C) to 55.4% (90 °C). Meanwhile, the rate constants increased by more than 50-fold as temperature increased from 30 °C to 90 °C **(Fig. S11a, SI)**, indicating that the br-PFOS degradation in S^{2-}/VB12 system is endothermic. In order to calculate the apparent activation energy, Arrhenius plot was fitted as shown in **Fig. S11b, SI**. A good linear correlation ($r^2 = 0.96$) was achieved between T^{-1} and $\ln k_{obs}$, indicating that the temperature effect adheres to the Arrhenius equation ($k = Aexp(-E_a(RT)^{-1})$). Based on the temperature dependence of the measured rate constants, the overall apparent activation energy (E_a) was calculated to be 62.86 kJ/mol. This value is slightly higher than that obtained in the photoreductive decomposition of PFOA with hydrated electrons (59.54 kJ/mol) [61], but much lower than that of PFOA pyrolysis (154 ± 11 kJ/mol) [62]. **Kim and Carraway** indicated that the activation energy could be lowered by ~ 40–60 kJ/mol in the presence of VB12 for the dichlorination of PCE [63]. However, although in the presence of the catalyst, efficient degradation and defluorination of br-PFOS still requires high temperatures. Therefore, new approaches are desired to activate C − F bond and further lower the activation energy of PFASs defluorination.

3.4.2. Effect of pH

pH is one of the most important environmental factors that affects the degradation of pollutants, and determines the sulfur forms by mediating the hydrolysis process. The effect of pH on the degradation and defluorination of br-PFOS by S^{2-}/VB12 system is shown in Fig. 5 **(c, d)**. The initial solution pH was adjusted with HCl solution to 3.68, 6.08, 7.03, 8.25, 11.28 and 12.27(unadjusted), respectively. As is shown in Fig. 5, when the initial pH was unadjusted (pH 12.27), br-PFOS can undergo effective degradation and defluorination, with 20-d degradation and defluorination ratios of 78.9% and 49.1%, respectively. When the initial solution pH was adjusted to 11.28, the 20-d degradation and defluorination ratios of br-PFOS decreased dramatically to 12.2% and 8.9%, respectively. Further pH decrease below 11.28 resulted in much lower degradation and defluorination ratios. At the initial pH of 3.68, 6.08, 7.03, and 8.25, the 20-d degradation ratios of br-PFOS were 3.9%, 5.2%, 5.8% and 6.9%, respectively, and the corresponding 20-d defluorination ratios were 0.8%, 2.4%, 3.2% and 4.1%, respectively. Therefore, as the initial solution pH increases in the range of 3.68–12.27, the degradation and defluorination ratios of br-PFOS increase accordingly. While the dramatic increase between pH 11.28 and 12.27 is noteworthy. The strong acceleration of the reaction at pH close to the pKa_2 of H_2S (as shown in **Fig. S12, SI**) shows that S^{2-} is the reactive sulfur species for the catalytic degradation and defluorination of br-PFOS. This may be attributed to the higher nucleophilicity and reducing strength of S^{2-} compared to HS^- and H_2S. The sulfur species with higher nucleophilicity were reported to have higher reaction rate constants with VB12 [57].

Besides the sulfur form, pH also affects the solution redox potential **(Fig. S13, SI)**. As the solution pH increased from 3.68 to 12.27, the redox potential decreased from −331.0 mV to −569.0 mV. The redox potential of VB12 is also strongly dependent on pH: a value of + 0.20 V (22 ◦C, NHE) remains independent in the region between pH 2.9 and 7.8 and moves to more negative values above pH 7.8 [64]. However, the pH dependence of the redox potential cannot explain the dramatic efficiency difference between pH 11.28 and pH 12.27. Therefore, we think that the sulfide form (unprotonated) instead of the redox potential determines PFOS degradation and defluorination efficiency under different pH conditions. Only S^{2-}, which has a higher nucleophilicity

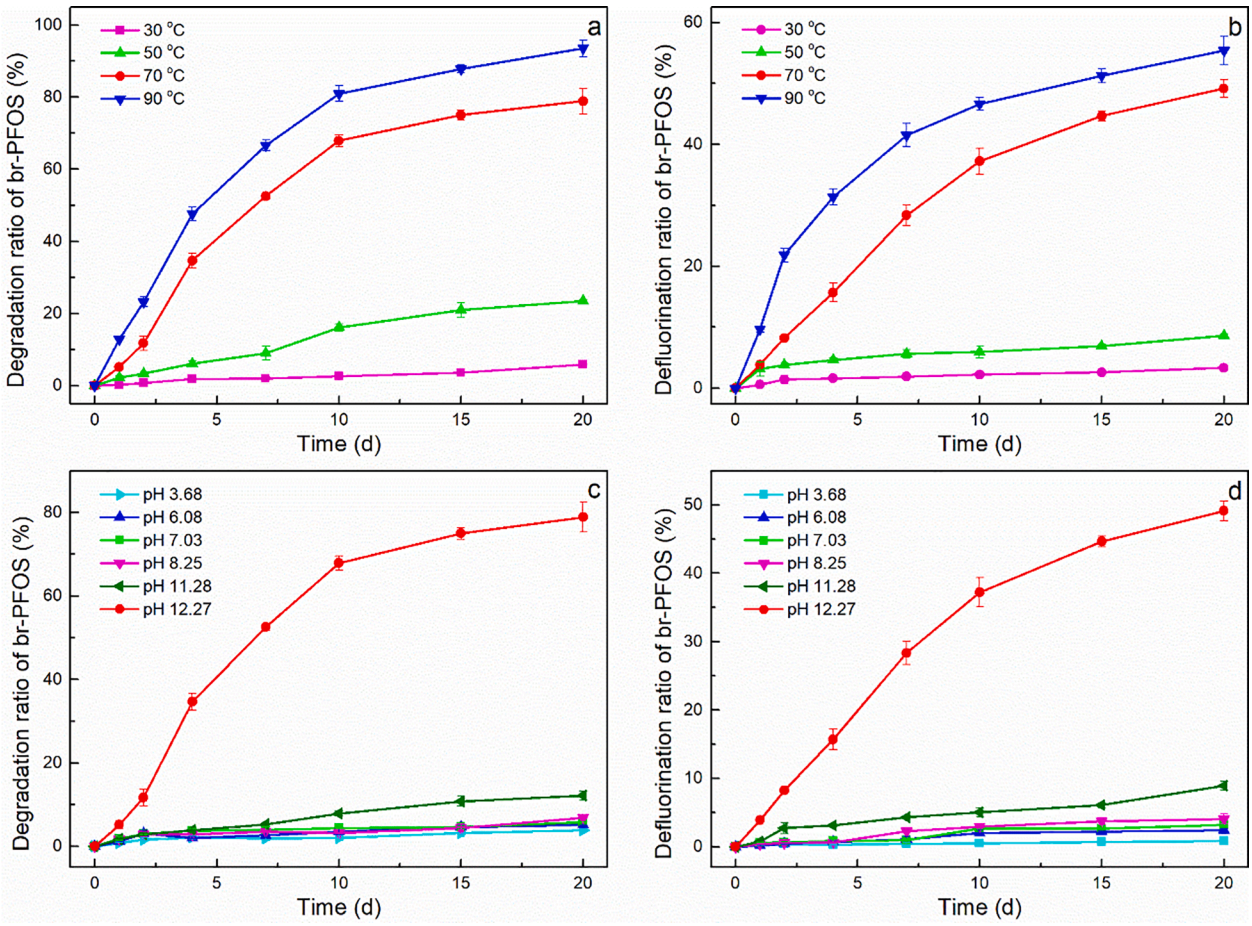

Fig. 5. Effect of temperature (**a, b**) and pH (**c, d**) on the degradation and defluorination of br-PFOS. Other conditions were identical with Fig. 1.

than HS^- and H_2S, can promote effective decomposition of br-PFOS in the presence of VB12.

3.4.3. *Effects of Na_2S and VB12 concentration*

The effect of Na_2S concentration on the degradation and defluorination of br-PFOS is shown in Fig. S14 **(a, b), SI**. As the Na_2S concentration increased from 1 mM to 100 mM, the 20-d degradation ratio of br-PFOS increased from 26.1% to 97.9%, and the 20-d defluorinaiton ratio of br-PFOS increased from 5.4% to 78.1%. The concentration increase of reducing agent can enhance the electron transfer between the reductant and catalyst, improve the turnover rate of VB12, and in turn accelerate the catalytic degradation and defluorination of br-PFOS. To be noted, there is an obvious improvement when Na_2S concentration increased from 10 mM to 30 mM. This can be explained by the complexation process of VB12. **Salnikov et al.** investigated the kinetics and mechanisms of VB12 reduction by sulfur-containing reducing agents in aqueous solutions and they ascribed the non-linear concentration dependence to the character of the rate-determining step [65]. When reducing agents are in excess, the rate-determining step is the elimination of the ligand; while at lower concentrations of reducing agents, it is their addition to cobalamin. Therefore, we chose 30 mM as the experimental Na_2S concentration, which is considered to be in excess for VB12 reduction.

The concentration of VB12 also has a great effect on the degradation and defluorination of br-PFOS (Fig. S14**c, d**). The pseudo-first-order rate constants for br-PFOS degradation were 0.0221 ± 0.0014 d^{-1}, 0.0342 ± 0.0013 d^{-1}, 0.0984 ± 0.0034 d^{-1}, 0.1251 ± 0.0049 d^{-1} and 0.165 ± 0.0090 d^{-1}, respectively, when the VB12 concentration was 30 μM, 100 μM, 300 μM, 600 μM and 1000 μM (Fig. S15**d**). When VB12 concentration increased from 100 μM to 300 μM, the br-PFOS degradation ratio increased greatly by 1.6-fold. Therefore, in our study we chose 300 μM as the optimal VB12 concentration.

4. Conclusions

1) Branched PFOS can be effectively decomposed and defluorinated in the presence of 300 μM VB12 and 30 mM S^{2-} at the temperature of 70 °C and pH of 12.3 under anoxic condition, with a pseudo-first-order kinetic rate constant of 0.0984 ± 0.0034 d^{-1}; while L-PFOS remained stable during 30 d reaction process. Both VB12 and S^{2-} are essential for br-PFOS decomposition.

2) The UV–Vis spectral characterization results indicate that VB12 (Co^{III}) can be reduced to Co^{II} by S^{2-} at ambient temperature and VB12 (Co^{II}) can initiate the reductive degradation and defluorination of br-PFOS. The latter is the rate-limiting step for the whole process. Effective br-PFOS decomposition can also occur with other common reductants such as dithiothreitol and L-cysteine which can reduce VB12 to Co^{II} as well. This implies abiotic/biological defluorination of br-PFOS are likely to occur in natural environment.

3) Based on the products detection, br-PFOS undergoes decomposition via H/F exchange, 2F β elimination, nucleophilic substitution of F by OH^-, C − C scission, C − S cleavage and *DHEH* pathway, with the formation of F^- and polyfluorinated sulfonates and carboxylates. Different from the VB12-nZn^0 system, HF/2F elimination followed by C − C scission is the dominant degradation pathway instead of the stepwise H/F exchange. This may be resulted from the Co^{II} oxidation state and strong alkaline condition of S^{2-}/VB12 system.

4) Temperature and pH have significant impacts on br-PFOS degradation and defluorination. Although with VB12 as the catalyst, high degradation efficiency relies on high temperatures (≥70 °C) due to the

high apparent activation energy of 62.86 kJ/mol. pH influences the reaction rate via determining the sulfide form rather than simply affecting the redox potential. S^{2-} instead of HS^- and H_2S is the reactive reductant. Na_2S and VB12 concentrations also have impacts on the degradation and defluorination of br-PFOS.

5. Environmental implications

This study revealed for the first time that VB12(Co^{II}) can initiate the reductive defluorination of br-PFOS as well as VB12(Co^{I}), which means that the catalytic degradation of br-PFOS by VB12 can be accomplished at a relatively high redox potential, and thereby there will be more alternatives for the reductant besides the strong artificial ones like Ti(III)-citrate and nanoscale zero-valent metals. Furthermore, the reductive degradation pathways of br-PFOS differ in various VB12 systems and strong alkaline condition may favor the deep defluorination and C–C scission of br-PFOS.

However, given the high temperature and pH requirement and the inefficiency of current VB12 systems in catalyzing the transformation of L-PFOS, development of new VB12 catalytic systems that can further lower the activation energy and improve the catalytic ability is desirable. For instance, some synergistic and heterogeneous catalytic systems, such as VB12/photocatalysis [66], VB12/dehalogenases [56], etc., have been reported to have synergistic catalytic effects on the dehalogenation of organic halides. Additionally, although the dechlorination and debromination mechanisms have been studied intensively, the catalytic mechanism [67,68], interaction mode [22,69,70] and regioselectivity [71] of VB12 are different in regard to various halogenated substrates. Therefore, in-depth studies on the catalytic defluorination mechanism of VB12 are also needed.

Declaration of Competing Interest

The authors declare that they have no known competing financial interests or personal relationships that could have appeared to influence the work reported in this paper.

Acknowledgements

This study has been supported by the National Natural Science Foundation of China (Project No. 21906016, 21976135, 21677109), the Fundamental Research Funds for the Central Universities (No. 2232020D-25) and the State Key Laboratory of Pollution Control and Resource Reuse Foundation (No. PCRRF19007).

Declaration of interests

We declare that we have no actual or potential conflict including financial, personal or other relationships with other people or organizations within three years of beginning the submitted work that could inappropriately influence, or be perceived to influence, their work.

Appendix A. Supplementary data

Supplementary data to this article can be found online at https://doi.org/10.1016/j.cej.2021.130149.

References

[1] E. Kissa, Fluorinated surfactants and repellents, CRC Press, 2001.
[2] J.P. Giesy, K. Kannan, Peer reviewed: perfluorochemical surfactants in the environment, Environmental science & technology 36 (7) (2002) 146A–152A.
[3] R. Renner, Growing Concern Over Perfluorinated Chemicals, Environ. Sci. Technol. 35 (7) (2001) 154A–160A, https://doi.org/10.1021/es012317k.
[4] A.G. Paul, K.C. Jones, A.J. Sweetman, A First Global Production, Emission, And Environmental Inventory For Perfluorooctane Sulfonate, Environ. Sci. Technol. 43 (2) (2009) 386–392, https://doi.org/10.1021/es802216n.
[5] S.C. Agency, Occurrence and use of highly fluorinated substances and alternatives, KEMI 361 (164) (2015).
[6] S.B. Nash, S.R. Rintoul, S. Kawaguchi, I. Staniland, J. van den Hoff, M. Tierney, R. Bossi, Perfluorinated compounds in the Antarctic region: Ocean circulation provides prolonged protection from distant sources, Environmental Pollution 158 (9) (2010) 2985–2991.
[7] C. Lau, K. Anitole, C. Hodes, D. Lai, A. Pfahles-Hutchens, J. Seed, Perfluoroalkyl acids: A review of monitoring and toxicological findings, Toxicological Sciences 99 (2) (2007) 366–394.
[8] NIEHS, National Institutes of Environmental Health Sciences, 2018. https://factor.niehs.nih.gov/2018/3/science-highlights/pfas/index.htm. March 18.
[9] H. Hori, E. Hayakawa, H. Einaga, S. Kutsuna, K. Koike, T. Ibusuki, H. Kiatagawa, R. Arakawa, Decomposition of Environmentally Persistent Perfluorooctanoic Acid in Water by Photochemical Approaches, Environ. Sci. Technol. 38 (22) (2004) 6118–6124, https://doi.org/10.1021/es049719n.s001.
[10] S. Park, J.E. Zenobio, L.S. Lee, Perfluorooctane sulfonate (PFOS) removal with Pd-0/nFe(0) nanoparticles: Adsorption or aqueous Fe-complexation, not transformation? J. Hazard. Mater. 342 (2018) 20–28.
[11] J.S.C. Liou, B. Szostek, C.M. DeRito, E.L. Madsen, Investigating the biodegradability of perfluorooctanoic acid, Chemosphere 80 (2) (2010) 176–183.
[12] H. Moriwaki, Y. Takagi, M. Tanaka, K. Tsuruho, K. Okitsu, Y. Maeda, Sonochemical decomposition of perfluorooctane sulfonate and perfluorooctanoic acid, Environmental Science & Technology 39 (9) (2005) 3388–3392.
[13] H. Lin, J.F. Niu, S.Y. Ding, L.L. Zhang, Electrochemical degradation of perfluorooctanoic acid (PFOA) by Ti/SnO2-Sb, Ti/SnO2-Sb/PbO2 and Ti/SnO2-Sb/MnO2 anodes, Water Research 46 (7) (2012) 2281–2289.
[14] Z. Zhang, J.J. Chen, X.J. Lyu, H. Yin, G.P. Sheng, Complete mineralization of perfluorooctanoic acid (PFOA) by gamma-irradiation in aqueous solution, Sci Rep 4 (2014) 6.
[15] Y.C. Lee, S.L. Lo, P.T. Chiueh, D.G. Chang, Efficient decomposition of perfluorocarboxylic acids in aqueous solution using microwave-induced persulfate, Water Research 43 (11) (2009) 2811–2816.
[16] Z. Sun, C. Zhang, L. Xing, Q. Zhou, W. Dong, M.R. Hoffmann, UV/Nitrilotriacetic Acid Process as a Novel Strategy for Efficient Photoreductive Degradation of Perfluorooctanesulfonate, Environmental science & technology 52 (5) (2018) 2953–2962.
[17] H. Hori, Y. Nagaoka, A. Yamamoto, T. Sano, N. Yamashita, S. Taniyasu, S. Kutsuna, I. Osaka, R. Arakawa, Efficient decomposition of environmentally persistent perfluorooctanesulfonate and related fluorochemicals using zerovalent iron in subcritical water, Environmental science & technology 40 (3) (2006) 1049–1054.
[18] K. Yasuoka, K. Sasaki, R. Hayashi, An energy-efficient process for decomposing perfluorooctanoic and perfluorooctane sulfonic acids using dc plasmas generated within gas bubbles, Plasma Sources Sci. Technol. 20 (3) (2011) 7.
[19] N. Assafanid, K.F. Hayes, T.M. Vogel, Reductive dechlorination of carbon-tetrachloride by cobalamin(ii) in the presence of dithiothreitol - mechanistic study, effect of redox potential and pH, Environmental Science & Technology 28 (2) (1994) 246–252.
[20] C.J. Gantzer, L.P. Wackett, Reductive dechlorination catalyzed by bacterial transition-metal coenzymes, Environmental Science & Technology 25 (4) (1991) 715–722.
[21] N. Assafanid, L. Nies, T.M. Vogel, Reductive dechlorination of a polychlorinated biphenyl congener and hexachlorobenzene by vitamin-b12, Applied and Environmental Microbiology 58 (3) (1992) 1057–1060.
[22] K.A.P. Payne, C.P. Quezada, K. Fisher, M.S. Dunstan, F.A. Collins, H. Sjuts, C. Levy, S. Hay, S.E.J. Rigby, D. Leys, Reductive dehalogenase structure suggests a mechanism for B12-dependent dehalogenation, Nature 517 (7535) (2015) 513-+.
[23] B. Yang, J.P. Deng, L.Y. Wei, Y.N. Han, G. Yu, S.B. Deng, C.Z. Zhu, H.B. Duan, Q. F. Zhuo, Synergistic effect of ball-milled Al micro-scale particles with vitamin B-12 on the degradation of 2,2 ',4,4 '-tetrabromodiphenyl ether in liquid system, Chem. Eng. J. 333 (2018) 613–620.
[24] S.D. Copley, Microbial dehalogenases: enzymes recruited to convert xenobiotic substrates, Curr. Opin. Chem. Biol. 2 (5) (1998) 613–617.
[25] D.B. Janssen, J.E. Oppentocht, G.J. Poelarends, Microbial dehalogenation, Curr. Opin. Biotechnol. 12 (3) (2001) 254–258.
[26] V. Ochoa-Herrera, R. Sierra-Alvarez, A. Somogyi, N.E. Jacobsen, V.H. Wysocki, J. A. Field, Reductive defluorination of perfluorooctane sulfonate, Environmental science & technology 42 (9) (2008) 3260–3264.
[27] S. Park, C. de Perre, L.S. Lee, Alternate Reductants with VB12 to Transform C8 and C6 Perfluoroalkyl Sulfonates: Limitations and Insights into Isomer Specific Transformation Rates, Products and Pathways, Environmental Science & Technology 51 (23) (2017) 13869–13877.
[28] J.Y. Liu, D.J. Van Hoomissen, T.C. Liu, A. Maizel, X.C. Huo, S.R. Fernandez, C. X. Ren, X. Xiao, Y.D. Fang, C.E. Schaefer, C.P. Higgins, S. Vyas, T.J. Strathmann, Reductive Defluorination of Branched Per- and Polyfluoroalkyl Substances with Cobalt Complex Catalysts, Environ. Sci. Technol. Lett. 5 (5) (2018) 289–294.
[29] T.A. Lewis, M.J. Morra, P.D. Brown, Comparative product analysis of carbon tetrachloride dehalogenation catalyzed by cobalt corrins in the presence of thiol or titanium (III) reducing agents, Environmental Science & Technology 30 (1) (1996) 292–300.
[30] L.Y. Ying, Y.Y. Long, L.H. Yao, W.J. Liu, L.F. Hu, C.R. Fang, D.S. Shen, Sulfate reduction at micro-aerobic solid-liquid interface in landfill, Science of the Total Environment 667 (2019) 545–551.
[31] W.W. Ma, M.X. Zhu, G.P. Yang, T. Li, In situ, high-resolution DGT measurements of dissolved sulfide, iron and phosphorus in sediments of the East China Sea: Insights into phosphorus mobilization and microbial iron reduction, Marine Pollution Bulletin 124 (1) (2017) 400–410.

[32] S. Suominen, K. Doorenspleet, J.S.S. Damste, L. Villanueva, Microbial community development on model particles in the deep sulfidic waters of the Black Sea, Environ. Microbiol. 18.
[33] M.R. Kriegmanking, M. Reinhard, Transformation of carbon-tetrachloride in the presence of sulfide, biotite, and vermiculite, Environmental Science & Technology 26 (11) (1992) 2198–2206.
[34] T.A. Nguyen, R.S. Juang, Treatment of waters and wastewaters containing sulfur dyes: A review, Chem. Eng. J. 219 (2013) 109–117.
[35] E. Vaiopoulou, P. Melidis, A. Aivasidis, Sulfide removal in wastewater from petrochemical industries by autotrophic denitrification, Water Research 39 (17) (2005) 4101–4109.
[36] M. Gagol, R.D.C. Soltani, A. Przyjazny, G. Boczkaj, Effective degradation of sulfide ions and organic sulfides in cavitation-based advanced oxidation processes (AOPs), Ultrason. Sonochem. 58 (2019) 6.
[37] A.L. Roberts, P.M. Gschwend, Mechanism of pentachloroethane dehydrochlorination to tetrachloroethylene, Environmental Science & Technology 25 (1) (1991) 76–86.
[38] R.P. Schwarzenbach, W. Giger, C. Schaffner, O. Wanner, Groundwater contamination by volatile halogenated alkanes - abiotic formation of volatile sulfur-compounds under anaerobic conditions, Environmental Science & Technology 19 (4) (1985) 322–327.
[39] W.R. Haag, T. Mill, Some reactions of naturally-occurring nucleophiles with haloalkanes in water, Environmental Toxicology and Chemistry 7 (11) (1988) 917–924.
[40] J.E. Barbash, M. Reinhard, Abiotic dehalogenation of 1,2-dichloroethane and 1,2-dibromoethane in aqueous-solution containing hydrogen-sulfide, Environmental Science & Technology 23 (11) (1989) 1349–1358.
[41] P.L. Miller, D. Vasudevan, P.M. Gschwend, A.L. Roberts, Transformation of hexachloroethane in a sulfidic natural water, Environmental Science & Technology 32 (9) (1998) 1269–1275.
[42] N. Assaf-Anid, K.Y. Lin, Carbon tetrachloride reduction by Fe2+, S2-, and FeS with vitamin B-12 as organic amendment, J. Environ. Eng.-ASCE 128 (1) (2002) 94–99.
[43] R.C. Buck, J. Franklin, U. Berger, J.M. Conder, I.T. Cousins, P. de Voogt, A. A. Jensen, K. Kannan, S.A. Mabury, S.P.J. van Leeuwen, Perfluoroalkyl and polyfluoroalkyl substances in the environment: terminology, classification, and origins, Integrated environmental assessment and management 7 (4) (2011) 513–541.
[44] J.P. Benskin, A.O. De Silva, J.W. Martin, Isomer Profiling of Perfluorinated Substances as a Tool for Source Tracking: A Review of Early Findings and Future Applications, in: D.M. Whitacre, P. DeVoogt (Eds.), Reviews of Environmental Contamination and Toxicology, Vol 208: Perfluorinated Alkylated Substances, Springer, New York, 2010, pp. 111–160.
[45] I. Langlois, M. Oehme, Structural identification of isomers present in technical perfluorooctane sulfonate by tandem mass spectrometry, Rapid Commun. Mass Spectrom. 20 (5) (2006) 844–850.
[46] A. Karrman, K. Elgh-Dalgren, C. Lafossas, T. Moskeland, Environmental levels and distribution of structural isomers of perfluoroalkyl acids after aqueous fire-fighting foam (AFFF) contamination, Environmental Chemistry 8 (4) (2011) 372–380.
[47] Y. Li, X.M. Feng, J. Zhou, L.Y. Zhu, Occurrence and source apportionment of novel and legacy poly/perfluoroalkyl substances in Hai River basin in China using receptor models and isomeric fingerprints, Water Research 168 (2020) 11.
[48] S. Beesoon, J.W. Martin, Isomer-Specific Binding Affinity of Perfluorooctanesulfonate (PFOS) and Perfluorooctanoate (PFOA) to Serum Proteins, Environmental Science & Technology 49 (9) (2015) 5722–5731.
[49] J.M. O'Brien, A.J. Austin, A. Williams, C.L. Yauk, D. Crump, S.W. Kennedy, Technical-grade perfluorooctane sulfonate alters the expression of more transcripts in cultured chicken embryonic hepatocytes than linear perfluorooctane sulfonate, Environmental Toxicology and Chemistry 30 (12) (2011) 2846–2859.
[50] R.L. Sharpe, J.P. Benskin, A.H. Laarman, S.L. MacLeod, J.W. Martin, C.S. Wong, G. G. Goss, Perfluorooctane sulfonate toxicity, isomer-specific accumulation, and maternal transfer in zebrafish (*danio rerio*) and rainbow trout (*oncorhynchus mykiss*), Environmental Toxicology and Chemistry 29 (9) (2010) 1957–1966.
[51] M.J. Bentel, Y.C. Yu, L.H. Xu, Z. Li, B.M. Wong, Y.J. Men, J.Y. Liu, Defluorination of Per- and Polyfluoroalkyl Substances (PFASs) with Hydrated Electrons: Structural Dependence and Implications to PFAS Remediation and Management, Environmental Science & Technology 53 (7) (2019) 3718–3728.
[52] L. Jin, P.Y. Zhang, Photochemical decomposition of perfluorooctane sulfonate (PFOS) in an anoxic alkaline solution by 185 nm vacuum ultraviolet, Chem. Eng. J. 280 (2015) 241–247.
[53] D. Dolphin, B12 Volume 1: Chemistry, John Wiley & Sons New York (1982).
[54] P. Schrapers, S. Mebs, S. Goetzl, S.E. Hennig, H. Dau, H. Dobbek, M. Haumann, Axial Ligation and Redox Changes at the Cobalt Ion in Cobalamin Bound to Corrinoid Iron-Sulfur Protein (CoFeSP) or in Solution Characterized by XAS and DFT, PLoS One 11 (7) (2016) 20.
[55] J. Kim, C. Gherasim, R. Banerjee, Decyanation of vitamin B-12 by a trafficking chaperone, Proc. Natl. Acad. Sci. U. S. A. 105 (38) (2008) 14551–14554.
[56] R.Z. Liao, S.L. Chen, P.E.M. Siegbahn, Which Oxidation State Initiates Dehalogenation in the B12-Dependent Enzyme NpRdhA: Co-II, COI or Co-0? ACS Catal. 5 (12) (2015) 7350–7358.
[57] I.A. Dereven'kov, D.S. Salnikov, R. Silaghi-Dumitrescu, S.V. Makarov, O. I. Koifman, Redox chemistry of cobalamin and its derivatives, Coord. Chem. Rev. 309 (2016) 68–83.
[58] M.J. Bentel, Z.K. Liu, Y.C. Yu, J.Y. Gao, Y.J. Men, J.Y. Liu, Enhanced Degradation of Perfluorocarboxylic Acids (PFCAs) by UV/Sulfite Treatment: Reaction Mechanisms and System Efficiencies at pH 12, Environ. Sci. Technol. Lett. 7 (5) (2020) 351–357.
[59] T. Yamamoto, Y. Noma, S.-I. Sakai, Y. Shibata, Photodegradation of perfluorooctane sulfonate by UV irradiation in water and alkaline 2-propanol, Environmental Science & Technology 41 (16) (2007) 5660–5665.
[60] Y.R. Gu, W.Y. Dong, C. Luo, T.Z. Liu, Efficient Reductive Decomposition of Perfluorooctanesulfonate in a High Photon Flux UV/Sulfite System, Environmental Science & Technology 50 (19) (2016) 10554–10561.
[61] C.J. Zhang, Y. Qu, X. Zhao, Q. Zhou, Photoinduced Reductive Decomposition of Perfluorooctanoic Acid in Water: Effect of Temperature and Ionic Strength 43 (2) (2015) 223–228.
[62] P.J. Krusic, D.C. Roe, Gas-phase NMR technique for studying the thermolysis of materials: Thermal decomposition of ammonium perfluorooctanoate, Anal. Chem. 76 (13) (2004) 3800–3803.
[63] Y.H. Kim, E.R. Carraway, Reductive dechlorination of PCE and TCE by vitamin B-12 and ZVMs, Environ. Technol. 23 (10) (2002) 1135–1145.
[64] D. Lexa, J.M. Saveant, J. Zickler, Electrochemistry of vitamin B12. 2. Redox and acid-base equilibria in the B12a/B12r system, Journal of the American Chemical Society 99 (8) (1977) 2786–2790.
[65] D.S. Salnikov, I.A. Dereven'kov, E.N. Artyushina, S.V. Makarov, Interaction of cyanocobalamin with sulfur-containing reducing agents in aqueous solutions, Russ. J. Phys. Chem. A 87 (1) (2013) 44–48.
[66] H. Shimakoshi, Y. Hisaeda, Oxygen-Controlled Catalysis by Vitamin B-12-TiO2: Formation of Esters and Amides from Trichlorinated Organic Compounds by Photoirradiation, Angew. Chem.-Int. Edit. 54 (51) (2015) 15439–15443.
[67] B. Heckel, S. Cretnik, S. Kliegman, O. Shouakar-Stash, K. McNeil, M. Elsner, Reductive Outer-Sphere Single Electron Transfer Is an Exception Rather than the Rule in Natural and Engineered Chlorinated Ethene Dehalogenation, Environmental Science & Technology 51 (17) (2017) 9663–9673.
[68] S. Zhang, L. Adrian, G. Schueuermann, Dehalococcoides-Mediated B-12-Dependent Reductive Dehalogenation of Aromatics Does Not Proceed through Outer-Sphere Electron Transfer, Environmental Science & Technology 54 (24) (2020) 15751–15758.
[69] M. Semadeni, P.C. Chiu, M. Reinhard, Reductive transformation of trichloroethene by cobalamin: Reactivities of the intermediates acetylene, chloroacetylene, and the DCE isomers, Environmental Science & Technology 32 (9) (1998) 1207–1213.
[70] C. Kunze, M. Bommer, W.R. Hagen, M. Uksa, H. Dobbek, T. Schubert, G. Diekert, Cobamide-mediated enzymatic reductive dehalogenation via long-range electron transfer, Nat. Commun. 8 (2017) 11.
[71] S.W. Zhang, L. Adrian, G. Schuurmann, Interaction Mode and Regioselectivity in Vitamin B-12-Dependent Dehalogenation of Aryl Halides by Dehalococcoides mccartyi Strain CBDB1, Environmental Science & Technology 52 (4) (2018) 1834–1843.